

Relaxation of the nuclear magnetism of liquid ^3He at the surface of paramagnetic crystals

V. V. Naletov, M. S. Tagirov, D. A. Tayurskiĭ, and M. A. Teplov

V. I. Ulyanov (Lenin) State Univerity, Kazan, 420008 Russia

(Submitted 18 January 1995)

Zh. Éksp. Teor. Fiz. **108**, 577–592 (August 1995)

We present the results of experimental studies of the nuclear magnetic relaxation of ^3He atoms located in a narrow gap ($100\ \mu\text{m}$) between the pairs of crystals $\text{LiYF}_4\text{--LiYF}_4$ and $\text{LiYF}_4\text{--LiTmF}_4$. We propose a theoretical model to describe how the bounded geometry affects the relaxation rate of helium nuclei. The model allows us to qualitatively understand features in the relaxation process observed in experiments both with crystals and with powders. We show that an important role in the magnetic relaxation of helium is played by local nonuniformities in the magnetic field caused by defect paramagnetic ions of Tm^{3+} located at the walls of microcracks at the crystal surface. The experimental data show no evidence that resonant magnetic coupling between ^3He and ^{169}Tm influences the relaxation rate of magnetization of liquid helium-3. © 1995 American Institute of Physics.

1. INTRODUCTION

In recent years, a topic of particular interest in the study of the magnetic properties of liquid ^3He has been the magnetic relaxation of the liquid in contact with solids.^{1–7} The anomalously small thermal resistance (Kapitza resistance) observed almost thirty years ago at the boundary between liquid ^3He and cerium magnesium nitrate (Ref. 8) for $T < 10\ \text{mK}$ has stimulated the active study of magnetic properties of liquid ^3He in contact with solids. Friedman *et al.*¹ reliably established that liquid ^3He mediates a magnetic coupling between the spins of fluorine ^{19}F nuclei contained in microspheres of finely dispersed ($0.2\ \mu\text{m}$) DLX-6000 polytetrafluoroethylene powder, while Van Keuls *et al.*⁷ observed a transfer of magnetization from the nuclear spins of ^{19}F to protons contained in microspheres of polystyrene via the nuclear spins of liquid helium-3.

Despite intensive efforts over a period of thirty years, a full understanding of the mechanism for magnetic coupling is not yet at hand. We note that this question has an even longer history: even in the work of Romer⁹ it was established that the container walls affected the spin relaxation of helium-3.

At present, there are many ongoing experimental studies of the magnetic coupling between the nuclear spins of helium-3 and solid-state magnetic moments, in a variety of systems.^{1–7} In all of these experiments, in order to obtain a well-developed contact surface between the helium-3 and the solid-state substrate, the latter has been made in the form of solid powders, porous amorphous materials, porous polymers, etc. As exceptions we should note Refs. 10, whose authors studied the magnetic coupling between liquid helium and crystals of thulium ethylsulfate, and Ref. 11, where the helium was in contact with solid-state layers of nitrogen adsorbed at the surface of the CaF_2 and graphite epoxy. It is obvious that the use of disordered systems, e.g., solid powders, in these experiments must complicate the interpretation of the experimental data to a considerable degree,¹² and per-

haps wash out certain manifestations of the magnetic coupling between the liquid ^3He and the solid.

For example, a well developed surface necessitates treatment of the properties of the adsorbed layers of helium-3. According to Hammel and Richardson,¹³ fluctuations develop in the dipole fields of helium-3 atoms on the surface because helium-3 atoms are exchanged between the liquid in the volume and the solid-phase surface layer. This is responsible for the effective interaction between the ^3He nuclear magnetic moments and the magnetic moments of the solid body. We can therefore assume that the magnetic coupling between the magnetic moments of the liquid and the nuclear spins of the ^{19}F in Refs. 1 and 3 is brought about by the atoms of the adsorbed helium-3 layers.

Thus, any attempt to interpret the experimental data on magnetic relaxation of liquid helium-3 in contact with a solid must take into account at least three factors:

- a) the existence of magnetic moments (electronic or nuclear) in the solid adjacent to the helium-3;
- b) the effect of adsorbed solid-state layers of helium-3; and
- c) the limited size of the spaces between the solid particles in which the helium-3 atoms can move.¹⁴

The goal of this paper is to investigate the magnetic relaxation of liquid ^3He in contact with crystals of the Van Vleck paramagnet LiTmF_4 , which contains nuclear magnetic moments of ^{169}Tm whose gyromagnetic ratios are close to those of ^3He , and in contact with LiYF_4 , the diamagnetic analogue of LiTmF_4 . The smallness of the surface over which the crystal and liquid helium-3 are in contact allows us to exclude from consideration the effect of adsorbed solid-state layers of helium-3; furthermore, by using a single crystal we can reduce the effect of nonuniformities to a minimum in the corresponding processing of the surface (see Sec. 2.1).

Note also that most studies of magnetic relaxation of helium-3 in contact with a solid have been made at very low temperatures ($< 0.5\ \text{K}$). At these temperatures, liquid helium-3 is a degenerate Fermi liquid, and its kinetic prop-

erties can be described in terms of Landau Fermi liquid theory using the language of elementary excitations. Thus, for example, the elementary relaxation process for the longitudinal magnetization is the decay of a spin wave with zero wave vector into two spin waves with opposite nonzero wave vectors.

In contrast, we made our measurements in the temperature range from 1.5 to 3 K, where liquid helium-3 is a non-degenerate quantum liquid for which the Landau theory is not applicable. In this range, liquid helium-3 possesses a number of interesting properties due to its large zero-point vibrational energy;¹⁵⁻¹⁷ moreover, it is probably necessary to include the effect of real motion of ^3He atoms on the magnetic relaxation (see Sec. 5).

2. EXPERIMENTAL SETUP

2.1. Samples

At this time, out of the entire class of insulating Van Vleck paramagnets the two best-studied crystals are thulium ethyl sulfate (TmES) and lithium thulium double fluoride (LiTmF_4) (see, e.g., Ref. 18). Both crystals possess comparatively high (axial) symmetry, and are characterized by strong anisotropy of the γ tensor of the ^{169}Tm nuclei. Because their spins equal 1/2, there is no need to take into account quadrupole effects on the magnetic relaxation. All of these facts make these two materials very attractive from the standpoint of comparing the results of experimental studies of the kinetics of liquid ^3He spins in contact with a crystal surface with theoretical representations and calculations. In the first experiments of Ref. 10, a single crystal of thulium ethyl sulfate was used, allowing the authors to observe the existence of resonant magnetic coupling between ^{169}Tm nuclei and nuclei in a fine layer (0.1 mm) of liquid ^3He coating the entire surface of a cylindrical sample of TmES ($h=3$ mm, $d=3$ mm). When the external magnetic field \mathbf{H}_0 was directed at an angle of 7° from the c axis of the crystal, the Zeeman splitting of the thulium nuclei was the same as that of the helium-3. The difference in the nature of the magnetism made it possible to distinguish spin echo signals from ^{169}Tm (probe pulse lengths 1 and 2 μs , spin-spin relaxation time $T_2=25$ μs) and those of the liquid ^3He nuclei (probe pulse lengths 10 and 20 μs , $T_2=25$ μs). One of the most successful experiments revealed that the time T_1 for the spin-lattice relaxation of liquid ^3He nuclei decreases from 6.5 to 2.4 s when the gyromagnetic ratios of thulium and helium-3 are exactly equal. Subsequently Richardson and his coworkers observed a similar effect, namely, cross-relaxation between ^3He and the nuclei of solid ^{14}N ($I=1$) adsorbed on the surface of CaF_2 and graphite epoxy.¹¹

We do not use the term "successful experiment" idly here. The fact is that the crystal hydrate $\text{Tm}(\text{C}_2\text{H}_5\text{SO}_4)_3 \cdot 9\text{H}_2\text{O}$ is chemically unstable when exposed to vacuum, particularly the surface. The state of the latter is practically impossible to reproduce from trial to trial, which in turn affects the overall reproducibility of the phenomena under study. This desire to have complete reproducibility of results from trial to trial is the reason why all subsequent experiments, including ours, have used the chemically stable

crystalline compound LiTmF_4 . In addition, there was some hope initially that resonance effects in the magnetic coupling could be enhanced by replacing single crystal samples of lithium thulium double fluoride by magnetically oriented powders of LiTmF_4 . With regard to magnetic properties these materials are analogous to single-crystal LiTmF_4 ; furthermore, what is very important, they offer the major advantage of a well-developed crystal surface.⁵

In a certain sense, these hopes bore fruit: anisotropy was observed in the relaxation of the longitudinal magnetization of the nuclei of liquid ^3He in the pores of magnetically oriented LiTmF_4 powder with particle sizes <57 μm , <20 μm , 2–4 μm , and <1 μm . These experiments, however, did not supply direct proof of the influence of cross-relaxation.

Analysis of the experimental results for single crystals of TmES and magnetically oriented LiTmF_4 powders lead us to conclude that it is necessary to investigate liquid ^3He in the simplest possible sample geometries and with close monitoring of the surface quality. The structure of our experimental cell will be described below in Sec. 2.2; here we will present data from studies of surface layers of polished single crystals of LiYF_4 .¹⁹

Mechanical processing (cutting, grinding, and polishing) gives rise to structural damage in the near-surface layers of the crystal; this damage takes many forms and extends to a considerable depth. A layer of damaged crystal with uncontrollable thickness is undesirable, because it leads to imperfect reproducibility of the experimental results. The primary problem in making a layer-by-layer analysis is to choose the correct polishing etch for a given crystal layer. Our studies have shown the following:

- 1) for uniform removal of layers of the crystal LiYF_4 , the most suitable etch is an aqueous solution of KOH saturated at 60° ;
- 2) the isolation of surface defects (selective etching) is best carried out with solutions of H_2SO_4 and HNO_3 ; and,
- 3) for cleaning a surface of contaminants, solutions containing H_2O_2 and HF can be used.

By combining methods of mechanical, chemical, and ion-beam etching and monitoring the surface of LiYF_4 crystals by optical microscopy, microhardness, and electron diffraction in "reflection," we were able to obtain surfaces of single crystals of the double fluorides with structures close to those of the bulk crystal. In this case, we estimated that the depth of the surface defects (scratches) was at most 100 μm .

According to EPR data, our LiTmF_4 crystals contained the following paramagnetic impurities: Nd^{3+} (0.023% with respect to the Tm^{3+} ions) and Nd^{3+} (0.007%). In crystals of LiYF_4 the impurity concentration was 3 to 4 times smaller.

2.2. Experimental cell

Figure 1 shows a sketch of the experimental cell we used in this work to measure pulsed NMR of liquid ^3He . The two single crystals ($\text{LiTmF}_4\text{--LiYF}_4$ and $\text{LiYF}_4\text{--LiYF}_4$), which were cylindrical in shape, (diameter 6.0 mm and height 6.0 mm), were fitted tightly into a cylindrical container made of "Stycast 1266" epoxy resin; in this case the c -axis of the

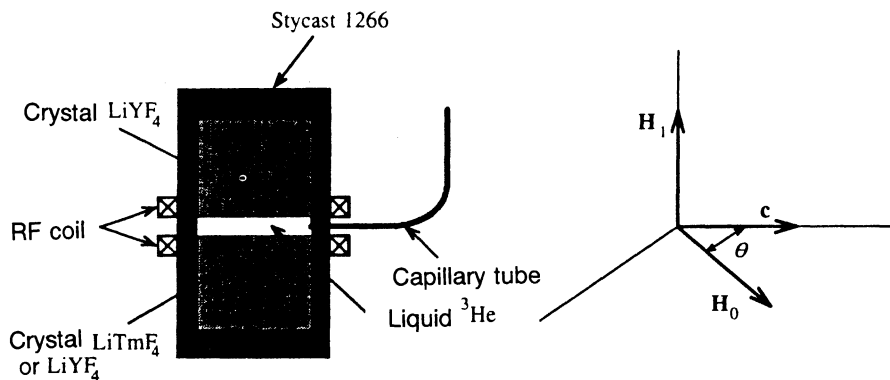


FIG. 1. Experimental cell.

crystal was directed along the cylinder diameter. Liquid ^3He was condensed into the plane-parallel $100\ \mu\text{m}$ gap between the carefully polished crystal surfaces through a capillary made of stainless steel. In the experiments with pure ^3He , impurities of the commoner isotope ^4He were less than 0.04%. The constant magnetic field H_0 was oriented in the plane of the gap, in one case parallel and in the other case perpendicular to the c -axis. The magnetic field H_0 at the center of the electromagnet ($1\ \text{cm}^3$) was uniform to about $5 \cdot 10^{-5}$, and the long-period stability was better than 10^{-5} .

The rf coil was mounted directly on the exterior wall of the container, which at the time of the experiments was in a bath of liquid ^4He at temperatures in the range 1.5–4.2 K.

2.3. Measurement method

Because of the comparatively small volume of liquid helium-3 in the gap between the crystals ($V=5 \cdot 10^{-5}\ \text{cm}^3$), and hence the small number of resonating nuclear spins of helium-3 ($4.5 \cdot 10^{19}$), the signal/noise ratio in our experiments was rather low (5/1). However, with the help of a high-speed digital accumulator used for laboratory preparations¹⁾ based on a PC AT-286/287, we were able to measure the relaxation parameters to an accuracy of better than 4%.

In our work, we used the pulse sequence $\pi/2 - \tau - \pi/2 - \tau_1 - \pi - \tau_1 - \text{echo}$. to measure the longitudinal relaxation time for the magnetization of ^3He nuclei: In all the experiments, the time dependence of magnetization was described by the expression

$$M = M(\infty)[1 - \exp(-\tau/T_1)]. \quad (1)$$

Our measurements of the transverse relaxation times of the ^3He nuclei were based on the falloff in the spin-echo amplitude $M(2\tau_1)$ as the delay time τ_1 between the $\pi/2$ - and π -probe pulses was increased. In all the experiments, we were able to describe the evolution of the transverse magnetization by the expression

$$M(2\tau_1)/M(0) = \exp[-(2\tau_1/T_2)^n]. \quad (2)$$

The values of T_2 and n were determined by the method of least squares; in this case, the exponent varied from 1 to 3 depending on the experimental conditions.

3. EXPERIMENTAL RESULTS

3.1. NMR of thulium

The signal from free-induction decay of the thulium ^{169}Tm nuclei was observed in the temperature interval from 1.5 to 4.2 K at a frequency of 5.9 MHz with the magnetic field H_0 oriented along the crystallographic c -axis. The temperature dependence obtained, which is shown in Fig. 2, is well approximated by the expression

$$T_1^{-1} = 3.4T^{1.5} + 4 \cdot 10^7 \exp(-47.5/T), \quad (3)$$

where the first term is due to relaxation of thulium nuclei via paramagnetic impurities (see Sec. 2.1),²⁰ while the second is from fluctuations of the hyperfine magnetic field created by the $4f$ shell of the Tm^{3+} ions.²¹ The exponent in expression (3) is in good agreement with the value of the energy of the first excited doublet in the crystal LiTmF_4 .²²

3.2. NMR of liquid helium-3

We measured the longitudinal and transverse relaxation times for nuclei of liquid helium-3 in the LiYF_4 – LiYF_4 gap at a temperature of 1.5 K in a magnetic field of 2.41 kOe, and in the LiTmF_4 – LiYF_4 gap at a temperature of 1.5 K and

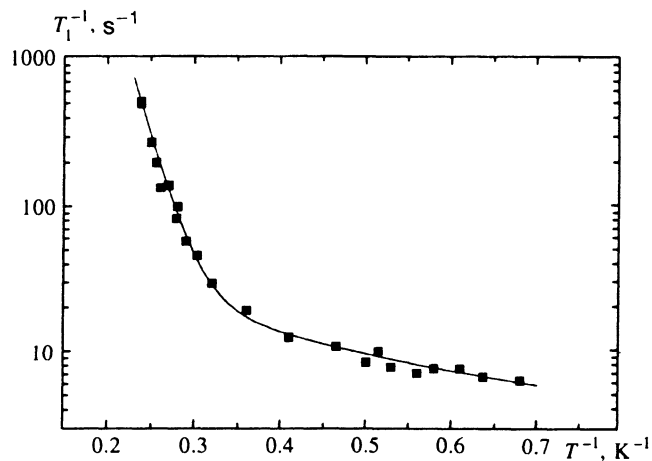


FIG. 2. Temperature dependence of longitudinal relaxation rate of ^{169}Tm nuclei in a single crystal of LiTmF_4 with the magnetic field orientation $H_0 \parallel c$. The solid curve is calculated using Eq. (3)

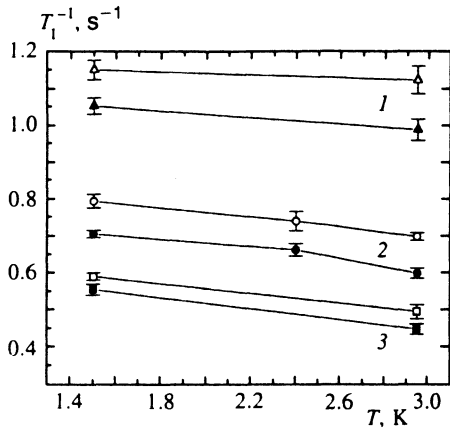


FIG. 3. Temperature dependence of the longitudinal relaxation rate of nuclei of liquid ^3He in the $\text{LiYF}_4\text{-LiTmF}_4$ gap for $H_0 = 6.1$ kOe (1), 2.4 kOe (2), and 1.9 kOe (3). The light dots are for $H_0 \parallel c$, the dark dots are for $H_0 \perp c$.

2.95 K in magnetic fields 1.19, 2.41, and 6.1 kOe (the corresponding resonance frequencies for the ^3He nuclei were 3.86, 7.82, and 19.8 MHz). These fields were applied along various directions: along the c -axis of the crystal LiTmF_4 , as well as perpendicular to this axis and at an angle of 7.4° to the c -axis (for this orientation of the magnetic field the effective gyromagnetic ratio of the thulium ^{169}Tm nucleus coincides with that of the ^3He nucleus). We note at once that we observed no cross-relaxation effects of the sort observed in Ref. 10 when the magnetic field H_0 was oriented at an angle of 7.4° to the c -axis.

In addition, the magnetic relaxation of liquid ^3He was studied at a temperature of 1.5 K in $^3\text{He-}^4\text{He}$ solutions (the relative concentration of the ^4He was $\leq 0.04\%$, 0.4%, 5%, 20%, 40%, and 80%, the last of which corresponds to a superfluid solution). The principal results of the measurements are given in Figs. 3–5 and Table I.

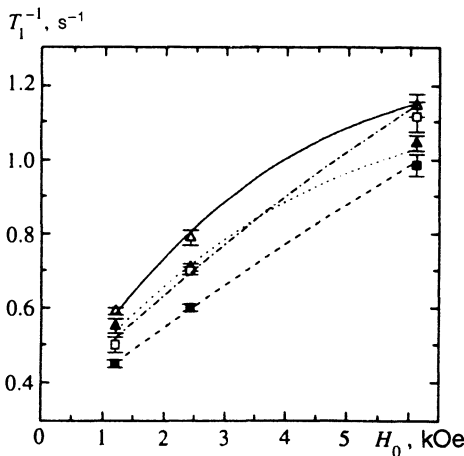


FIG. 4. Dependence of the rate of longitudinal relaxation for liquid ^3He nuclei on the value of the external magnetic field H_0 in the $\text{LiYF}_4\text{-LiTmF}_4$ gap. Notation: Δ —1.5 K, $H_0 \perp c$; \square —2.95 K, $H_0 \perp c$; \blacktriangle —1.5 K, $H_0 \parallel c$; \blacksquare —2.95 K, $H_0 \parallel c$.

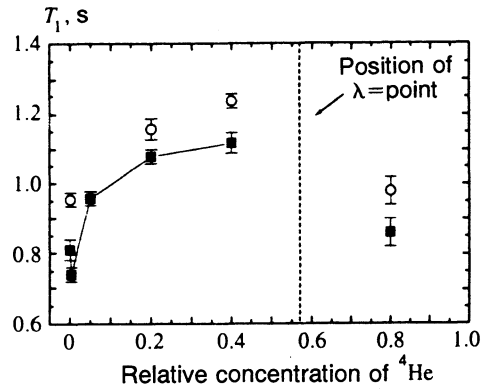


FIG. 5. Dependence of the longitudinal relaxation time of liquid ^3He nuclei in the $\text{LiYF}_4\text{-LiTmF}_4$ gap on the concentration of ^4He ; $T = 1.5$ K, $f = 19.8$ MHz. The light dots are for $H_0 \parallel c$, the dark dots are for $H_0 \perp c$.

4. DISCUSSION OF EXPERIMENTAL RESULTS

4.1. Relaxation of liquid helium-3 nuclei in contact with diamagnetic crystals of LiYF_4

We observed rather short longitudinal and transverse relaxation times for nuclear spins of liquid helium-3 ($T_1 = 7$ s, $T_2 = 5.8$ ms) in contact with diamagnetic LiYF_4 crystals. Let us first analyze the transverse relaxation. This short decay time for the transverse magnetization of ^3He nuclei could only be caused by magnetic field gradients in the gap between the crystals. Since diamagnetic LiYF_4 crystals do not contain intrinsic electronic magnetic moments capable of creating a macroscopic field between the crystal boundaries, and the content of magnetic impurities in our samples was small (see Sec. 2.1), the only source of a magnetic field gradient is nonuniformity of the field of the electromagnet (see Sec. 2.2). In order to compare the transverse relaxation time of ^3He nuclei in the $\text{LiYF}_4\text{-LiYF}_4$ gap with that for nuclei in the $\text{LiYF}_4\text{-LiTmF}_4$ gap, we measured T_2 for the same values of nonuniformity of the external magnetic field. This enabled us to distinguish the various contributions to T_2^{-1} .

Our measured value of the longitudinal relaxation rate was unexpectedly large under these experimental conditions. It was always an order of magnitude smaller than the relaxation rate of liquid ^3He observed in experiments with the helium in contact with solid-state particles of submicron size,⁵ and two orders of magnitude larger than the rate of longitudinal relaxation of nuclei in bulk liquid helium,⁹ where the magnetization of ^3He relaxes via modulation of the dipole-dipole interactions, which is caused by diffusive motion. In our case, the magnetization of the liquid helium nuclei can be transferred either to the Zeeman reservoir of paramagnetic impurities or to the reservoir of exchange motion of ^3He atoms in the solid-state film adsorbed at the crystal surface.¹³

Let us estimate whether it is possible for impurity paramagnetic ions contained in the crystals to affect the longitudinal relaxation of liquid helium. In order for the impurity paramagnetic ions and the helium nuclei to be in thermal contact (which leads to flipping of the helium nuclear spins

because of fluctuations in the magnetization of impurity atoms), it is necessary that a certain condition hold between the magnetic heat capacities of helium-3 C_{He} and of the impurity atoms C_{imp} , namely

$$C_{\text{He}} T_1^{-1} = C_{\text{imp}} T_{1,\text{imp}}^{-1} \quad (4)$$

Calculations show that, for these impurity concentrations (see Sec. 2.1) and all reasonable values of the spin-lattice relaxation rate $T_{1,\text{imp}}^{-1}$ for the impurities, it is impossible to satisfy Eq. (4) even in order of magnitude.

Thus, these two mechanisms do not explain the observed value of the relaxation rate. Since the measured value of the rate is rather close to that of longitudinal relaxation of liquid ^3He nuclei in contact with solid powder,⁵ it is sensible to seek an explanation for our experiments in terms of the processes that occur near the surface of the LiYF_4 crystals. A characteristic shared by single crystal and powders made of single crystal particles is that nonuniformities smaller than $100 \mu\text{m}$ remain at the surface of a single crystal (see Sec. 2.1) even after processing. Naturally these same nonuniformities are present at the surface of single-crystal particles, but in the latter case there are more of them, since the overall particle surface is larger than the surface of the single crystal. It is reasonable to assume that these microcracks are fractal in character, like the cracks at the surface of metals.²³

Figure 6 shows a possible form for these irregularities, which we are provisionally calling "fractal pits." Hence the following longitudinal relaxation mechanism is entirely reasonable: the magnetization of the nuclei of the bulk liquid helium is rapidly (over times of order T_2) communicated via diffusive processes to helium nuclei in microcracks. There, as shown in Sec. 5, the spectral composition of the diffusive motion changes because of the bounded geometry, and relaxation occurs due to modulation of dipole-dipole interactions mediated by the motion of the helium atoms. The same relaxation mechanism occurs in LiYF_4 powder (sample V in Ref. 5).

4.2. Relaxation of liquid helium-3 nuclei in contact with the crystals LiYF_4 – LiTmF_4

Replacement of one of the diamagnetic LiYF_4 crystals by a crystal of the Van Vleck paramagnet LiTmF_4 results in a significant increase in the rates of both transverse and longitudinal relaxation of the magnetization of liquid helium nuclei. Furthermore, anisotropy now appears in the relaxation parameters of the liquid helium, which reflects the magnetic property of the substrate.

Table I records our measurements made under the same conditions as in the LiYF_4 – LiYF_4 system (the FWHM width of the spin echo was $30 \mu\text{s}$ in a field of 2.4 kOe). These measurements clearly record the appearance of an additional source of magnetic field gradient, which, however, does not affect the integrated width of the spin echo. Our calculations show that the Van Vleck magnetization of the crystal LiTmF_4 cannot create the required nonuniformity of the magnetic field in the LiYF_4 – LiYF_4 gap since our maximum computed value of magnetic field fluctuation at a distance of $5 \mu\text{m}$ is about 0.5 Oe per centimeter. It is therefore reasonable to assume that the sources of these local magnetic

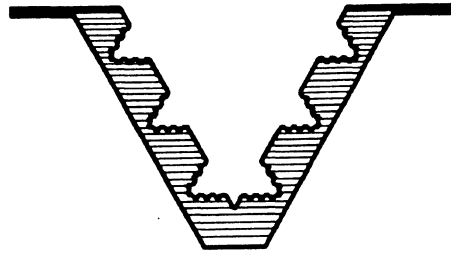


FIG. 6. Possible shape of microcrack structures at the surface of the crystal (the surface profile follows a Koch curve).

field gradients are paramagnetic Tm^{3+} ions located at the walls of microcracks²⁾ (we assume that the surfaces of the LiTmF_4 and LiYF_4 crystals are structurally equivalent). The different values of the transverse relaxation rate of the liquid helium-3 nuclei for perpendicular and parallel orientations of the field H_0 indicate that the magnetic susceptibility of defect paramagnetic Tm^{3+} centers is anisotropic.

Let us discuss how the proposed mechanism can explain the temperature and field dependences of the longitudinal relaxation rate for liquid helium-3 nuclei. Note first that the observed temperature and field dependence cannot be explained by means of traditional approaches, i.e., relaxation into a reservoir of spin-spin interactions among paramagnetic impurities, direct transfer of magnetization from liquid helium nuclei to resonating nuclei in the substrate, or relaxation into a reservoir of exchange motions of helium atoms in the adsorbed solid-state film. The last mechanism is ineffective because of the smallness of the surface over which the helium is in contact with in the crystal. In our experiments, the only nuclei to which ^3He spins can directly transfer their magnetization are ^{169}Tm nuclei, whose spin-lattice relaxation rate decreases with decreasing temperature (see (3)). Furthermore, the magnetic specific heat of the surface Van Vleck Tm^{3+} ion nuclei is insufficient to ensure thermal contact.

As for relaxation through paramagnetic impurities, aside from their low surface density, this mechanism gives rise to reversed temperature and field dependences.²⁶ The following relaxation mechanism is the most likely one. As in the experiments with the diamagnetic LiYF_4 – LiYF_4 crystals, diffusive processes cause the magnetization of the bulk liquid helium-3 to quickly reach the ^3He nuclei immediately adjacent to the surface of the LiTmF_4 crystals. The relaxation of the longitudinal magnetization is responsible for the motion of the helium-3 atoms in microcracks on the surface, as in the case of diamagnetic crystals. However, in a bounded geometry (the "fractal pits") this motion occurs in a magnetic field which is locally very nonuniform in consequence of the paramagnetic thulium ion defects located in the pit walls.

On the other hand, this nonuniformity enhances helium relaxation processes in the wells. (Reference 27 treated a somewhat similar situation: longitudinal relaxation of the magnetization of particles moving in a randomly fluctuating magnetic field. This motion causes the relaxation rate to increase as the field strength rises and the temperature drops. Our experiments display a similar tendency. But this model cannot be employed directly here because, first, the field of

TABLE I. Transverse relaxation parameters of ^3He nuclei.

Samples	$T = 1.5 \text{ K}$		$T = 2.95 \text{ K}$	
	$\mathbf{H}_0 \parallel \mathbf{c}$	$\mathbf{H}_0 \perp \mathbf{c}$	$\mathbf{H}_0 \parallel \mathbf{c}$	$\mathbf{H}_0 \perp \mathbf{c}$
LiTmF ₄ - LiYF ₄	$T_2 = 5.47(6) \text{ ms},$ $n = 2.4(1)$	$T_2 = 1.74(3) \text{ ms},$ $n = 2.2(1)$	$T_2 = 4.5(1) \text{ ms},$ $n = 2.3(1)$	$T_2 = 1.40(3) \text{ ms},$ $n = 2.1(4)$
LiYF ₄ - LiYF ₄	$T_2 = 5.8(3) \text{ ms},$ $n = 1$			

the defect ions is highly anisotropic, and secondly, liquid helium-3 has a number of special properties, noted in Sec. 5.) On the other hand, the nuclear spins of the helium atoms have different Zeeman frequencies in such nonuniform magnetic fields, which impedes the exchange of magnetization between such atoms. Thus, the effectiveness of the mechanism will be determined by competition between two processes: the enhancement of relaxation in nonuniform magnetic fields and the exchange of magnetization between helium atoms in the layer at the surface.

In terms of this mechanism we also can interpret data on relaxation of the longitudinal magnetization of helium-3 nuclei in ^3He - ^4He solutions. When ^4He is added, atoms of ^4He will be found predominantly in the microcracks due to the differing values of the Van der Waals interaction with atoms of the substrate wall. Therefore, the penetration of ^3He atoms into the microcracks will be more and more impeded as the concentration of helium-4 increases, and the rate of longitudinal relaxation of ^3He will decrease. We note that the concentration dependence of T_1^{-1} (Fig. 5) is very reminiscent of the adsorption curve of ^4He in ^3He - ^4He solutions.²⁸ As the superfluid state is approached, this constraint on admission of helium-3 atoms to the microcracks is lifted, and the rate of ^3He relaxation increases until it reaches values measured in pure helium-3.

5. MODEL OF RELAXATION IN A BOUNDED GEOMETRY

In this section we estimate theoretically the effect of a bounded geometry on the magnetic relaxation of liquid ^3He nuclei, using the model of spherical pores in a solid. In this case we should keep in mind the following facts. Relaxation of ^3He in a bounded geometry turns out to be affected both by the size and shape of the pores, as well as the fraction of ^3He atoms located near the surface of the solid. Here we are interested only in how the size of the spherical pores in the solid affects the magnetic relaxation of liquid ^3He .

According to the classical theory of Bloembergen, Purcell, and Pound,²⁹ the longitudinal (T_1^{-1}) and transverse (T_2^{-1}) relaxation rates of magnetic moments in the liquid arising from modulation of the dipole-dipole interaction by diffusive motion are equal, and are determined by the expression

$$T_1^{-1} = T_2^{-1} = \frac{2\pi N\gamma^4\hbar^2}{5dD}, \quad (5)$$

where N is the density of the magnetic moments, γ is their gyromagnetic ratio, D is the diffusion coefficient, and d is the distance of closest approach for atoms or molecules that possess a magnetic moment. For ^3He the values of N , γ , and

D are known: $N \approx 1.55 \cdot 10^{22} \text{ cm}^{-3}$, $\gamma = -2\pi \cdot 3241 \text{ Hz/Oe}$, and $D = 10^{-4} \text{ cm}^2/\text{s}$ for $T \approx 1 \text{ K}$, whereas d can only be estimated from indirect data. It is reasonable to choose as an estimate for d in liquid ^3He a distance slightly larger than the diameter of an atom. Then from Eq. (5) we obtain $T_1^{-1} = T_2^{-1} \approx 800 \text{ s}$, which is in good agreement with observed experimental relaxation times in bulk ^3He liquid at a temperature of $\approx 3 \text{ K}$.⁹ The generalization of the Bloembergen *et al.* expression to the case of lower temperatures (below the Fermi degeneracy temperature) was given in Ref. 30.

On the other hand, the experimentally measured longitudinal and transverse relaxation times for nuclei of liquid ^3He in a bounded geometry between solid-phase particles are considerably shorter and differ from one another. Equation (5) therefore does not yield the right order of magnitude for the relaxation times and cannot account for the difference.

We will assume that the mechanism for magnetic relaxation of ^3He nuclear moments in the pores of solid-state powders remains the same as in the theory of Bloembergen *et al.* and try to take into account size effects due to the bounded geometry. It is not difficult to see why the boundedness of the geometry can affect the magnetic relaxation time from the following qualitative considerations. In a solid, where there is practically no translational motion of the atoms, the magnetic resonance line is rather broad and the transverse relaxation time small. In liquids, the translational motion of the atoms causes a strong narrowing of the resonance line, and the relaxation time is long. When a liquid in which modulation of the dipole-dipole interaction by diffusive motion is a significant relaxation mechanism is in a bounded region (e.g., a spherical pore) instead of a bulk liquid, some types of diffusive motion are no longer possible: only resonant modes "fsurvive." Consequently, the magnetic resonance curve will not be as severely pinched as in the case of the bulk liquid, nor as broad as in the case of a solid body. For helium-3 in this temperature range such limitations on the diffusive motion may be even greater, e.g., on account of the Pauli exclusion principle. Unfortunately, at present there are only rough thermodynamic models for describing liquid helium-3 at temperatures above the Fermi-degeneracy temperature,¹⁷ and so we will treat it here as a nonquantum liquid.

It is obvious that size effects need to be included only when an atom of helium is able to reach the walls of the pore and, perhaps, undergo several collisions with the walls within a magnetic relaxation time (here and in what follows we will consider pores of spherical shape and neglect the possibility of transfer of a helium atom to the next pore).

Then the radius of such a sphere is approximately equal to $R \approx \sqrt{DT_2} \approx 10^{-3}$.

In order to calculate the relaxation time using the theory of Bloembergen, Purcell, and Pound, we must solve the diffusion equation

$$\frac{\partial \Psi(\mathbf{r}, t)}{\partial t} = D \Delta \Psi(\mathbf{r}, t) \quad (6)$$

with the initial condition

$$\Psi(\mathbf{r}, 0) = \delta(\mathbf{r} - \mathbf{r}_0). \quad (7)$$

This solution has the form

$$\begin{aligned} \Psi(\mathbf{r}, t) &= \sum_{nlm} \frac{2(\mu_n^{(l)})^2}{\pi R^3 [1 + (\mu_n^{(l)})^2 - (l + 1/2)^2] [J_{l+1/2}(\mu_n^{(l)})]^2} j_l \\ &\times \left(\frac{\mu_n^{(l)} r_0}{R} \right) j_l \left(\frac{\mu_n^{(l)} r}{R} \right) Y_{lm}(\Omega_0) Y_{lm}(\Omega) \\ &\times \exp \left[-D \left(\frac{\mu_n^{(l)}}{R} \right)^2 t \right], \end{aligned}$$

where $Y_{lm}(\Omega)$ is the spherical harmonic of order l , Ω is the solid angle, and $j_l(z)$ is a spherical Bessel function of integer order l [$J_{l+1/2}(z) = \sqrt{2z/\pi} j_l(z)$], and μ_n^l is the n -th root of the equation

$$-J_{l+1/2}(z) + 2zJ'_{l+1/2}(z) = 0.$$

Then according to the theory of Bloembergen *et al.*, we have for the rate of relaxation of helium nuclei²⁹

$$\begin{aligned} T_1^{-1} &= \frac{9}{8} \gamma^4 \hbar^2 [J^{(1)}(\omega) + J^{(2)}(2\omega)], \\ T_2^{-1} &= \frac{3}{4} \gamma^4 \hbar^2 \left[\frac{15}{4} J^{(1)}(\omega) + \frac{3}{8} J^{(2)}(2\omega) + \frac{3}{8} J^{(0)}(0) \right], \end{aligned} \quad (8)$$

where $\omega = \gamma H_0$ is the Larmor frequency of the nuclear spins in the external field H_0 and $J^q(\omega)$ is the spectral intensity of the correlation function for the dipole-dipole interaction parameters. According to our calculations, this spectral intensity for the case of a spherical pore equals

$$\begin{aligned} J^{(q)}(\omega) &= \alpha^{(q)} \frac{4N}{DR} \sum_n \\ &\times \frac{[(R/d)^{3/2} J_{3/2}(\mu_n^{(2)} d/R) - J_{3/2}(\mu_n^{(2)})]^2}{(\mu_n^{(2)})^4 + \omega^2 \tau^2} \\ &\times \frac{(\mu_n^{(2)})^2}{((\mu_n^{(2)})^2 - 6) [J_{3/2}(\mu_n^{(2)})]^2}, \end{aligned} \quad (9)$$

where $\alpha^{(0)} = 48\pi/15$, $\alpha^{(1)} = 8\pi/15$, $\alpha^{(2)} = 32\pi/15$ and $\tau = R^2/D$ is a parameter playing the role of a correlation time. Calculations using Eqs. (8) and (9) show that, e.g., in a field $H_0 = 10$ kOe, the longitudinal and transverse relaxation times of liquid helium nuclei in a spherical pore with radius $R \approx 10^{-3}$ practically coincide with the values of the relaxation time for the bulk liquid. This remains true down to very small pore dimensions. However, for pore dimensions less

than 100 Å (which corresponds to residual nonuniformities at the surface of our crystals after processing) the effects of the bounded geometry begin to be felt. For $R = 50$ Å the parameter τ becomes very small—of order 10^{-9} s, so that we have $\omega\tau \ll 1$ for the fields we used and Eq. (9) simplifies considerably:

$$\begin{aligned} J^{(q)}(\omega) &= \alpha^{(q)} \frac{4N}{DR} \sum_n \\ &\times \frac{[(R/d) j_1(\mu_n^{(2)} d/R) - j_1(\mu_n^{(2)})]^2}{(\mu_n^{(2)})^2}. \end{aligned} \quad (10)$$

The main contribution to the sum over n comes from the first few terms; estimates show that the transverse relaxation time becomes smaller than the longitudinal relaxation time by a factor of 1.2 to 1.6 in the interval 10 to 100 s, depending on the pore radius. For lower-symmetry pores (e.g., pores with cylindrical symmetry) we should expect the decrease in the values of the relaxation times to be even larger and the difference between T_1 and T_2 to increase.

Note also that Eqs. (8) and (10) imply that the relaxation rate is independent of the value of the magnetic field. However, Fig. 4 reveal our experiments with the crystals LiYF_4 – LiTmF_4 such a field dependence is observed. In the previous section we showed that this dependence can be explained by the existence of defect paramagnetic centers at the surface of the LiTmF_4 crystal. It is therefore interesting to study the field dependence of the magnetic relaxation rate of nuclear helium-3 spins within the LiYF_4 – LiYF_4 gap where defect paramagnetic centers are absent and acceleration of the relaxation of liquid ^3He nuclei can only be due to the bounded geometry.

6. RELAXATION OF ^3He NUCLEI AT THE SURFACE OF CRYSTALS AND MAGNETICALLY ORDERED POWDERS (COMPARISON)

It has been observed both in this work and in experiments on finely dispersed powders⁵ that when the helium is in contact with the surface of the Van Vleck paramagnet LiTmF_4 , relaxation of the longitudinal magnetization takes place more rapidly than in the same experiments with the diamagnet LiYF_4 . This is strong evidence for the existence of a magnetic coupling of ^3He to the substrate; hence, in order to unify these experimental data it is reasonable to recall the most important features of relaxation of helium in powders of LiTmF_4 at $T = 1.5$ K, as reflected in the following relations (the numbers in brackets denote the size of the powder particles, the labels \parallel and \perp denote directions along the external field relative to the c' -axis, i.e., the axis of primary orientation of powder particles):

$$T_{1\parallel} \ll T_{1\perp}, \quad (11a)$$

$$T_{1\parallel}(< 20 \mu\text{m}) \approx T_{1\parallel}(< 1 \mu\text{m}) \ll T_{1\parallel}(2-4 \mu\text{m}), \quad (11b)$$

$$T_{2\parallel}(< 1 \mu\text{m}) = 12 \mu\text{s} \ll T_{2\perp}(< 1 \mu\text{m}). \quad (11c)$$

As is clear, the time T_1 is significantly smaller only for $H_0 \parallel c'$, and only in those samples that contain a large num-

ber of particles with submicron dimensions and consequently have a well-developed surface. In this case the relaxation time T_2 is short as well. In a sample with particles smaller than $1 \mu\text{m}$, the time $T_{2\parallel}$ turns out to be even smaller than for ^{19}F nuclei in CaF_2 .²⁶ Since the magnetic moments of ^3He nuclei are smaller than those of fluorine, and the distance between them cannot be less than the distance between ^{19}F atoms in CaF_2 , we must assume that relaxation of the transverse magnetization of helium in a sample of submicron particles of LiTmF_4 takes place not only due to dipole-dipole interaction of the nuclear spins of helium with each other, but also due to the action of the fluctuating magnetic field exerted by the paramagnet surface. Furthermore, taking into account the extremely strong effect on the relaxation of helium nuclei [$T_{2\parallel}(<1 \mu\text{m})=12 \mu\text{s}$], we must assume that paramagnetic centers immediately adjacent to the surface of crystalline particles of the powder are the source of these fluctuating fields. Our experiments show that natural impurities such as Nd^{3+} , Gd^{3+} , and other rare-earth ions are not capable of producing the observed effects, so Tm^{3+} ions situated near the surface in sites with severely distorted symmetry and having large magnetic moments seem to us to be the most likely candidates for the role of acceptors.

Thus, a decisive role in the magnetization transport process is played by surface atoms of helium, which are well coupled to the near-surface system of paramagnetic centers of the crystal. Naturally, this can serve as a channel for nuclear relaxation of bulk helium only under conditions of rather rapid exchange in energy between the bulk and near-surface helium, i.e., in the presence of spin diffusion. In a field $\mathbf{H}_0 \perp \mathbf{c}'$ the Van Vleck magnetism of LiTmF_4 is very large; therefore, the helium is acted on by a strongly nonuniform field in the space between the powder particles (the gradients reach 100 Oe per pore dimension). Consequently, there must be a scatter in the Larmor frequencies of the helium nuclear spins, which breaks the coupling between helium nuclei in the bulk and helium nuclei in the immediate vicinity of the surface. Apparently, the observed properties (11a) and (11c) are a manifestation of this loss of coupling.

It is obvious that in experiments with powders we must take into account the role of the solid adsorbed film of helium at the well-developed surface of the sample. Therefore, the following question arises: what is the ratio of the contribution to the longitudinal relaxation rate of helium from quantum exchange at the surface of the substrate to the contribution from relaxation in the microcracks? Unfortunately, the available experimental data on powders is insufficient to arrive at any conclusions about the role of the solid-state layer. In experiments with very coarse powders ($< 57 \mu\text{m}$), addition of the isotope ^4He does not cause T_1 to increase, which suggests that relaxation due to exchange is ineffective in this case. On the other hand, in the experiments of Richardson et al. (see, e.g., Ref. 31) it was reliably established that a solid-state film of ^4He (1–2 monolayers) significantly hinders the process by which the longitudinal magnetization recovers. It is likely that the disagreement among these results arises because the sample with the biggest particles is too small.

7. CONCLUSIONS

In conclusion, we will formulate the fundamental conclusions of this work:

1. The coupling of bulk ^3He to a magnetic substrate is mediated by atoms of ^3He at the surface and near the surface of the crystal (in microcracks at the surface of powder particles and single crystals).

2. The motion of these helium atoms is sufficiently different from the motion in the crystal in the liquid bulk that there is no averaging of the dipole-dipole interaction of the ^3He spins.

3. A nonuniform magnetic field (in particular, caused by Van Vleck magnetism) prevents the exchange of magnetization between the bulk and near-surface helium, so that the relaxation of the nuclei in the bulk liquid is slowed down. This implies that at temperatures of order 1.5 K the primary role in the transport of magnetization is played by spin diffusion of ^3He .

4. The experimental data do not contradict (but also do not confirm) the existence of resonant magnetic coupling (cross-relaxation) of nuclei of ^3He and ^{169}Tm . It is possible that this coupling is less efficient than that of relaxation processes in the local nonuniform fields of the microcracks.

5. In order to correctly compare the effectiveness of this mechanism with a mechanism involving participation of the solid state film, it is necessary to investigate further the kinetics of the magnetization of helium-3 in ^3He – ^4He solutions in the pores of magnetically oriented powders of LiTmF_4 .

This work was carried out with the support of the Russian Fund for Fundamental Research (project No. 93-02-2085). The authors are grateful to R. Yu. Abdulsabirov, S. L. Korablevoi, and V. A. Sakharov for preparing the samples, to I. N. Kurkin, I. Kh. Salikhov, and S. P. Kurzin for EPR studies in the crystals, and to A. V. Egorov for his interest in the work and a multitude of discussions.

¹)Designed by O. N. Bakharev.

²)It is well known that local distortions of the crystal field can fundamentally change the Stark structure of Van Vleck ions. Thus, instead of the traditional "nonmagnetic singlet-excited non-Kramers doublet" scheme, the lowered symmetry can cause the ground state of the term in the lower crystal field symmetry to be two closely spaced singlets (i.e., a quasidoublet). This picture²⁴ fits observations of LiTmF_4 crystals in which some of the thulium atoms are replaced by a rare-earth element with a different ionic radius. In our case, the most probable reason why defect paramagnetic Tm^{3+} centers appear is the lowered symmetry of the crystal field at the walls of the microcracks (the dashed portion shown in Fig. 6). EPR studies of Tm^{3+} defect ions in the analogous Van Vleck paramagnetic TmES argue in favor of this.²⁵

¹L. J. Friedman, P. J. Millet, and R. C. Richardson, *Phys. Rev. Lett.* **47**, 1078 (1981).

²R. C. Richardson, *Physica B* **126**, 298 (1984).

³S. Maegawa, A. Schuhl, M. W. Meisel, and M. Chapellier, *Europhys. Lett.* **1**, 83 (1986).

⁴O. Gonen, P. L. Kuhns, C. Zuo, and J. S. Waugh, *J. Magn. Res.* **81**, 491 (1989).

⁵A. V. Egorov, O. N. Bakharev, A. G. Volodin et al., *Zh. Éksp. Teor. Fiz.* **97**, 1175 (1990) [*Sov. Phys. JETP* **70**, 658 (1990)].

⁶I. S. Solodovnikov and N. V. Zavaritskii, *JETP Lett.* **56**, 162 (1992).

⁷F. W. Van Keuls, R. W. Singerman, and R. C. Richardson, *J. Low Temp. Phys.* **96**, 103 (1994).

- ⁸W. R. Abel, A. C. Anderson, W. C. Black, and J. C. Wheatly, *Phys. Rev. Lett.* **16**, 273 (1966).
- ⁹R. H. Romer, *Phys. Rev.* **115**, 1415 (1959); *Phys. Rev.* **115**, 1183 (1959).
- ¹⁰A. V. Egorov, F. L. Aukhadeev, M. S. Tagirov, and M. A. Teplov, *JETP Lett.* **39**, 480 (1984).
- ¹¹F. W. Van Keuls, T. J. Gramila, L. J. Friedman, and R. C. Richardson, **165-166**, 717 (1990).
- ¹²D. A. Tayurskii and M. S. Tagirov, *Appl. Magn. Res.* **6**, 587 (1994).
- ¹³P. C. Hammel and R. C. Richardson, *Phys. Rev. Lett.* **52**, 1441 (1984).
- ¹⁴D. A. Tayurskii, in *Extended Abstracts of the 28th AMPERE Congress*, p. 219 (Kazan, 1994).
- ¹⁵A. F. Andreev, *JETP Lett.* **28**, 556 (1978).
- ¹⁶A. M. Dyugaev, *Zh. Éksp. Teor. Fiz.* **87**, 1232 (1984) [*Sov. Phys. JETP* **60**, 704 (1984)]; *Zh. Éksp. Teor. Fiz.* **89**, 1220 (1985) [*Sov. Phys. JETP* **62**, 703 (1985)].
- ¹⁷A. M. Dyugaev, *J. Low Temp. Phys.* **78**, 79 (1990).
- ¹⁸L. K. Aminov and M. A. Teplov, *Usp. Fiz. Nauk* **147**, 49 (1985) [*Sov. Phys. Usp.* **28**, 762 (1985)].
- ¹⁹R. Yu. Abdulsabirov, S. L. Korableva, V. A. Sakharov, and M. S. Tagirov, *Surfaces: Physics, Chemistry, Mechanics* **10-11**, 125 (1994).
- ²⁰L. K. Aminov, M. S. Tagirov, and M. A. Teplov, *Zh. Éksp. Teor. Fiz.* **79**, 1322 (1980) [*Sov. Phys. JETP* **52**, 669 (1980)].
- ²¹L. K. Aminov, A. A. Kudryashov, M. S. Tagirov, and M. A. Teplov, *Zh. Éksp. Teor. Fiz.* **86**, 1791 (1984) [*Sov. Phys. JETP* **59**, 1042 (1984)].
- ²²H. P. Christensen, *Phys. Rev. B* **19**, 6573 (1979).
- ²³E. Lens, G. Ginea, and F. Flores, *Fractals' Physical Origin and Properties*, L. Pietronero (ed.), Plenum, New York (1989).
- ²⁴L. K. Aminov, A. V. Vinokurov, I. N. Kurkin *et al.*, *Phys. Stat. Solidi (b)* **152**, 191 (1989).
- ²⁵H. H. Dearman, *J. Chem. Phys.* **44**, 2218 (1966).
- ²⁶A. Abragam and M. Goldman, *Nuclear Magnetism: Order and Disorder*, Clarendon, Oxford (1982).
- ²⁷N. F. Fatkullin, *Zh. Éksp. Teor. Fiz.* **101**, 1561 (1992) [*Sov. Phys. JETP* **74**, 833 (1992)].
- ²⁸K. Thompson, *J. Low Temp. Phys.* **32**, 361 (1978).
- ²⁹A. Abragam, *Principals of Nuclear Magnetism*, Clarendon, Oxford (1961).
- ³⁰D. Vollhardt and P. Wölfle, *Phys. Rev. Lett.* **47**, 190 (1981).
- ³¹L. J. Friedman, T. J. Gramila, and R. C. Richardson, *J. Low Temp. Phys.* **55**, 83 (1984).

Translated by Frank J. Crowne